A New Physical Model for Life Time Prediction of Pb-free Solder Joints in Electromigration Tests

Tian Tian, A.M.Gusak*, O.Yu. Liashenko*, Jung-Kyu Han, Daechul Choi, and King-Ning Tu
Department of Materials Science and Engineering, UCLA
Los Angeles, California 90095-595, US
*Department of Theoretical Physics, Cherkasy National University, Cherkasy, Ukraine
+1-(310)-467-6872; tian85@ucla.edu

Abstract

We have employed high resolution synchrotron radiation x-rays 3D imaging techniques, both tomography and laminography, to study the electromigration (EM) failure mechanism in flip-chip solder joints. In these studies, the ex-situ imaging of the early-stage damage evolution at the interface between UBM and solder balls, revealed that the EM induced failure mode of solder joints could be described by Johnson-Mehl-Avrami (JMA) kinetics model. Thus, the JMA kinetics is proposed to serve as a new physical model for life-time prediction of Pb-free solder joints in EM tests. A corresponding Monte Carlo simulation was developed to investigate this simplified failure model and the dependence of the scale parameter and shape parameter in the statistical Weibull equation on the physical factors of the EM tests was studied.

Introduction

The void formation induced by EM at the cathode side is one of the most serious reliability concerns in the electronic packaging industry [1]. One key study in this field is how to predict the life time of the solder joints in the accelerated life tests within an acceptable testing time. Thus a reasonable modeling work basing on the real failure mechanism during accelerated EM tests, is valuable to be applied to make the life time prediction of the test vehicles under a certain stressing condition.

In the past few years, pancake-shape void formation and propagation was found to be the main failure mode of flip chip solder joints in the EM tests, since the unique line-to-bump geometry results in significant current crowding effect at the current entrance of the solder bumps. Accordingly, a few kinetics models describing the pancake-type void propagation has been built-up [2-4].

However, the main experimental evidences of the previous modeling works are SEM observations. Restricting the study of the flip chip joint to the traditional two-dimensional (2D) examination procedure can yield two problems. One is the difficulty in uncovering the kinetics in the real rest vehicle during EM, especially at the early stage, which requires nondestructively monitoring. The other one is that a 2D measurement will bring more uncertainties of the void growth measurement in a real three-dimensional (3D) structure. The both problems would result in the main limitation of the pancake-type void modeling works.

Recently, the applications of synchrotron based x-rays non-destructive 3D imaging techniques enabled us avoid the 2D problems just outlined. A couple of experiments have been done by our group. The quantitative ex-situ computed tomography study was conducted at beamline 8.3.2 at the Advanced Light Source (ALS) of Lawrence Berkeley National Laboratory (LBNL), to measure the effective charge number Z* of eutectic SnPb during EM tests precisely, by monitoring the dramatic growth of pre-existed voids inside the solder.[5] Moreover, the synchrotron-radiation computed laminography (SRCL), an alternatively 3D imaging technique, which is designed for flat samples, was employed to study the EM-induced voids formation and evolution at the interface between 7.5μm thick Cu UBM and SN100C(Sn, Cu (0.65%), Ni (500ppm), Ge (60ppm), Bi (110ppm), Pb (140 ppm)) solder bump[6], at the high energy beamline ID15A at the European Synchrotron Radiation Facility (ESRF). The imaging results showed that the mode of damage evolution at the interface was quite different from the failure mode of pancake-shape void formation and propagation model at the early stage. And the results were proposed to be fitted by JMA phase transformation theory. And an intrinsic link between JMA model and the Weibull distribution of life time was discussed.

Basing on the synchrotron radiation based x-rays 3D imaging observations, we propose that the JMA phase transformation model can serve as a new physical model for life time prediction of Pb-free solder joints in EM tests. In this letter, Monte Carlo simulation is employed to build up a simplified mathematical model of JMA induced failure. By investigating this model, we would like to study the dispersion of time-to-failures (TTFs) dependence on two physical parameters (nucleation frequency and growth velocity) and one geometrical parameter (the size of contact interface).

Experimental

A. Sample description

The figure 1(a) shows the test vehicle we used in this study provide by National Semiconductor Cooperation, a single printed circuit board (PCB) with 4 identical WL-CSP test chips labeled as U1, U2, U3, U4. The dimension of one chip is 3000μm×3000μm and consists of 36 solder balls. The diameter of each solder ball is 250 μm. The composition of the solder ball used here is SN100C. The flip chip configuration and dimension are shown by the figure 2(a), a schematic diagram of the cross-section of the sample tested.

B. EM test system in UCLA

To collect the life times of the test vehicles for statistical analysis, we conducted a series of the accelerated EM tests in UCLA. During the EM tests, the four test chips on a board were connected in series and current flowed through only one pair of bumps in each chip. When one of the four chips failed,

978-1-4673-1965-2/12/$31.00 ©2012 IEEE

a hook wire was soldered to bypass the failed chip and maintained the current flowed through the remaining chips. For example, if U2 failed (figure 1(a)), the TTF of U2 would be recorded, the failed unit would be bypassed and the subsequent EM test was pursued till all of the four chips are failed.

The EM tests were running with two different current densities: 7.5×10^{3} A/cm^{2} (low-current), and 1×10^{4} A/cm^{2} (high-current), at the same temperature 125°C. For each test condition, four test boards were tested (i.e. 16 test chips in series), thus there were 16 TTFs.

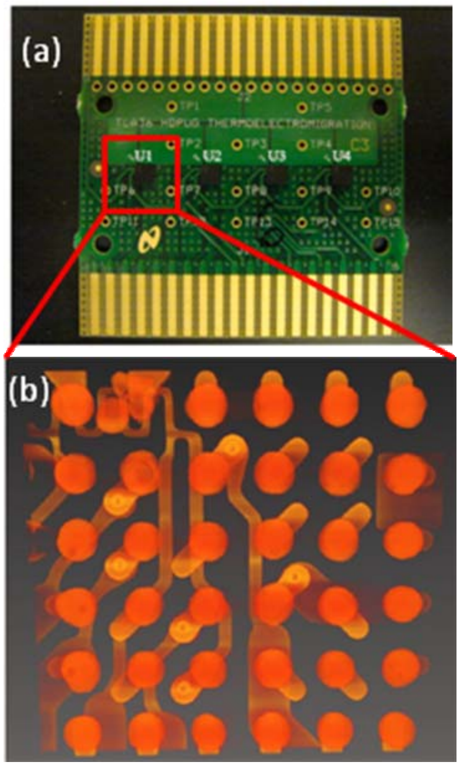

Figure 1 (a) a single test PCB with 4 test chips labeled as U1, U2, U3 and U4, (b) reconstructed micro-tomography 3D image of a failed test chips, with a melted solder ball at the upper left corner region.

C. Synchrotron radiation x-rays 3D imaging

One failed chip was imaged, shown in figure 1(b) by micro-tomography technique at beamline 8.3.2 at the ALS, LBNL. The principle of this technique has been described in detail elsewhere [7]. In this technique, the parallel x-rays with a beam size of 35mm (width) by 4.6 mm (height) passed through the sample that was mounted the rotation stage. The transmitted x-rays impinged on a 0.5 mm thick $CdWO_4$ single crystal scintillator that fluoresced the image as visible light that replayed via magnification lenses on the Cooke PCO 4000 CCD imaging camera (4008×2672 pixels). The contrast of the images comes from different attenuation lengths of metals caused by x-rays absorption. During data collection, the sample was rotated by 180^{0}C, in angular increments of 0.125^{0}, and an image recorded at each angular step with 1000ms exposure time. Reconstruction of the 3D images was conducted with Octopus software package from the University of Ghent. Viewing and analysis of the images were performed using the commercial 3-D visualization software Avizo 6.0. The voxel size used was 1.8µm, as set by the lens magnification and CCD pixel size. Figure 1(b) is the 3D tomography reconstructed image of one failure chip, showing that there are 36 bumps in the chip and the second bump on the upper left corner has failed by EM.

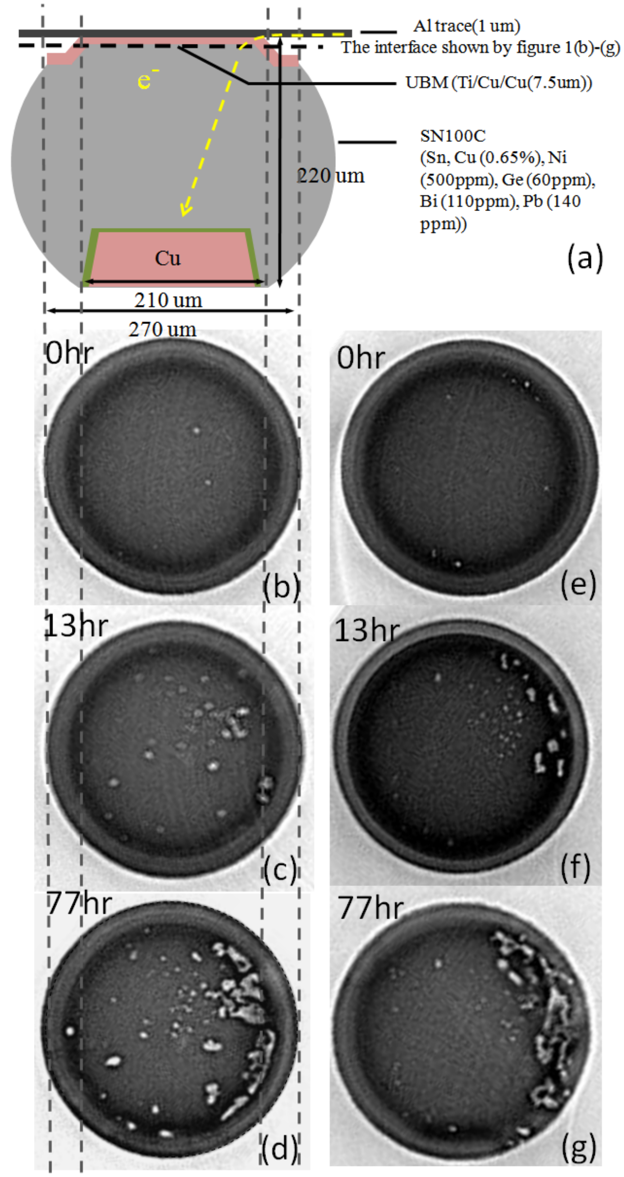

Figure 2(a) The schematic diagram of the cross-section of a tested solder joint, showing the configuration and dimensions of the sample. Figure 2(b)-(d) show the SRCL digital slice images of the sample I at the interface between the solder ball and the UBM before EM test (figure 2(b)), after 13 hr EM test(figure 2(c)), after 77 hr EM test(figure 2(d)), respectively, by 7.5×10^{3} A/cm^{2}, at 125°C. Figure 2(e)-(g) (Color online) show the SRCL digital slice images of the sample II at the interface between the solder ball and the UBM before EM test (figure 2(e)), after 13 hr EM test(figure 2(f)), after 77 hr EM test(figure 2(g)), respectively, by 1×10^{4} A/cm^{2}, at 125°C.[6]

To study the early damage evolution at the interface between UBM and solder ball, the ex-situ SRCL imaging experiments were conducted on the high energy beamline ID15A at the ESRF [6]. The general technique has been described elsewhere [8,9]. The main difference between laminography and tomography is that in the former one the rotation axis of the sample is not perpendicular to the x-ray beam and the algorithm is developed for imaging regions of interest (ROI) in flat, especially. Before the start of the accelerated EM tests, the solder joints were scanned for initial imaging in 3D as reference. After a given hours of EM stressing, the samples were re-scanned to check the changes inside. In the ex-situ SRCL imaging, two same chips were powered with the same two current densities: 7.5×10^3A/cm^2 (low-current), and 1×10^4A/cm^2 (high-current), and both were at the same temperature 125^{o}C, which is same as the one we used in the statistical study. Figure 2(b)-(d) show the digital slice images of the interface between the solder ball and UBM from top view at different time stages, which was stressed by low-current density. Similarly, figure 2(e)-(g) show the voids evolution at the top interface of the sample stressed by high-current density. The voxel size of the slice images is about 0.84μm.

Results and Discussion

A. Statistical analysis by Weibull Distribution

Statistical study of 16 TTFs with each EM condition has been carried. The cumulative distribution function (CDF) of the TTFs can be fitted by Weibull distribution [6]

$$F(t) = 1 - \exp\left(-\left(t/\eta\right)^{\beta}\right), \quad (1)$$

to get

1) η=619.3hr, β=2.34 under the high-current EM condition;
2) η=3471.8hr, β=1.8 under the low-current EM condition,

where η is the characteristic life time of the reliability under a certain testing condition, β is the shape parameter.

B. Physical analysis by JMA phase transformation model [6]

The SRCL imaging results, shown by figure 2(b-g), reveal that in real cases, the nucleation sites of voids are scattered on the interface at the early stage, even though later the growth rate of the voids in the current crowding region would be faster. This process is similar to the phenomenon of phase transformation described by JMA kinetics model [6],

$$X_T = 1 - \exp\left(-\left(t/\tau\right)^{n}\right), \quad (2)$$

where X_T is the degree of phase transformation at the time t, τ is the characteristic time of the transformation, and n is the parameter indicating the mode of new phase growth. Here we can define the degree of the void occupying at the interface $A_v/A_i=X_T$ and τ is the characteristic time of the voids growth. By measuring the voids area A_v at different time stage and whole interface area A_i, and thus fitting the relationship between $\ln\left(-\ln\left(1-X_T\right)\right)$: $\ln t$ linearly, we can get the value of both τ and n under each testing condition,

1) τ=768.5hr, n=0.7 under the high-current EM condition;
2) τ=3905.7hr, n=0.52 under the low-current EM condition.

C. Intrinsic link between Weibull distribution and JMA theory

From the above analysis, clearly, we found that equation (1) and (2) are in a same format and moreover the values of η and τ are in a good agreement, when they are under the same EM test condition. Thus, the nondestructive 3D imaging of the early stage void evolution at the interface between UBM and solder ball was proposed to be a rapid life prediction method, by applying the JMA kinetics model [6]. In our previous work, a simple explanation was provided to support the intrinsic link between JMA theory and Weibull distribution, even though they are used in two distinguished region: the link between these two models comes from the similarity as the weakest-link distribution in them.

D. Monte Carlo study on the model of "JMA induced mathematical failure"

The proposed application of JMA model in EM life time prediction bases on the observation of that the EM-induced failure of solder contact may be not caused by gradual propagation of one pancake void but instead by stochastic nucleation and lateral growth of many voids, when thinker UBMs are used. To understand this proposed model deeper, we start trying to investigate a very simplified mathematical model—"JMA induced mathematical failure". The model is built up with the following assumptions:

1) There are M solder contacts in the scheme and only one failure mode of these contacts: JMA nucleation and lateral growth of voids until full transformation of a contact into void.
2) Each nucleated circular island grows with constant velocity V, which is typical for JMA model.
3) The nucleation frequency per unit area ν is the same everywhere and constant in time.
4) The contact is a square area of L×L, where L is a side length.
5) The time of full coverage of void phase in a contact is treated as time-to-failure (TTF) in the simulation.

With the three mentioned physical parameters, V(m/s), υ(1/m^{2}s), L(m), we can introduce a non-dimensional parameter G=V/ υL^3. We suppose, this parameter, and only it, determines the statistics of TTFs. Due to existence of non-dimensional combination of three parameters, we can construct the characteristic time, characteristic length, and characteristic velocity in several ways. For example:

$$t_0 = \frac{1}{\nu L^2},\ l_0 = L,\ V_0 = \nu L^3 \ . \quad (3)$$

Here $t_0 = \frac{1}{\nu L^2}$ is an average time between successive nucleations in a whole contact area. Then non-dimensional time, length and velocity are

$$tt = \frac{t}{t_0} = \nu L^2 t,\ ll = \frac{l}{l_0},\ VV = \frac{V}{V_0} = \frac{V}{\nu L^3} \equiv G \cdot \quad (4)$$

Another possible choice is:

$$t_1 = \left(\frac{1}{\nu V^2}\right)^{1/3},\ l_1 = V t_1 = \left(\frac{V}{\nu}\right)^{1/3},\ V_1 = V \ \cdot \quad (5)$$

Here $t_1 = \left(\frac{1}{\nu V^2}\right)^{1/3}$ is an approximate time of covering an essential part of area. We can predict that the MTTF (meantime-to-failure) should be proportional to this characteristic time:

$$MTTF = zt_1 = z\left(\frac{1}{\nu V^2}\right)^{1/3}. \qquad (6)$$

Yet, we shall use the first choice (Eqs.(3,4)) of characteristic parameters since in numerical simulation it is more convenient to use the same non-dimensional size of the sample (in our case, square=1×1) and to change the non-dimensional velocity. So far we did not manage to solve this problem analytically, but the above introduced scaling allows us to obtain rather general results by the computed modeling of the non-dimensional problem.

The main points of the algorithm are as follow:

1) We treat the square sample ll×ll=1×1.
2) We divide both horizontal and vertical axes into N intervals, where $d_{xx}=d_{yy}=1/N$.
3) Each cell of area $d_{xx}\times d_{yy}=1/N^2$ can be in two states – “old” and “new”.
4) At each time step d_{tt}, all the elements of “old” state have a probability dp to transform to be that of “new” state, where

   $$dp = \nu dxdydt \equiv \frac{dx}{L}\frac{dy}{L}d\left(\nu L^2 t\right) = dxx\cdot dyy\cdot dtt = \frac{dtt}{N^2}$$

   Once an element (i,j) gets transformed, the time will be recorded as tt(i,j).
5) The successful nucleation site (i,j), at some time tt(i,j), becomes the center of transformation circle propagating with velocity VV=G, so that at any later time tt>tt(i,j) any cell in the circle of radius VV×(tt-tt(i,j)) with the center in cell (i,j) is obligatory “new”.
6) The time moment TTF(G), at which the last cell becomes new, is being written to memory as TTF(k;G), where k is a number of runs. After running the same program with the same non-dimensional velocity M times (1<k<M), we obtain an array of TTF, which could be statistically processed by standard code giving probability distribution (PDF), cumulative probability distribution (CDF) at given VV=G.
7) We change G in reasonable measures (0.1<G<5) and find the dependencies of Weibull CDF non-dimensional parameters a,b on G.

   $$F(tt) = 1-\exp\left(-\left(\frac{tt}{a}\right)^b\right),$$

   $$a = a(G=VV), b(G=VV).$$
8) Eventually we come back to parameters of Weibull distribution of real (in seconds) TTFs:

   $$F(t) = 1-\exp\left(-\left(\frac{t}{\eta}\right)^\beta\right),$$

   $$\beta = b,\quad \eta = a\cdot t_0 = a/\left(\nu L^2\right).$$

E. Results of the Monte Carlo Simulation

Figure 3 shows a typical example of the phase transformation process in our simulation, where VV=G=1, $d_{tt}=1$, $d_{xx}=d_{yy}=1/300$. In figure 3, the “old” phase is represented by blue color, and the “new” phase is represented by red. The typical non-dimensional TTF distribution and cumulative distributions for the set of parameters above are shown in figure 4. The dependence of parameters a, b as a function of non-dimensional parameter G=VV are shown in figure 5(a,b), with three different failure criteria(100%, 90% , and 80% “new” phase coverage, respectively).

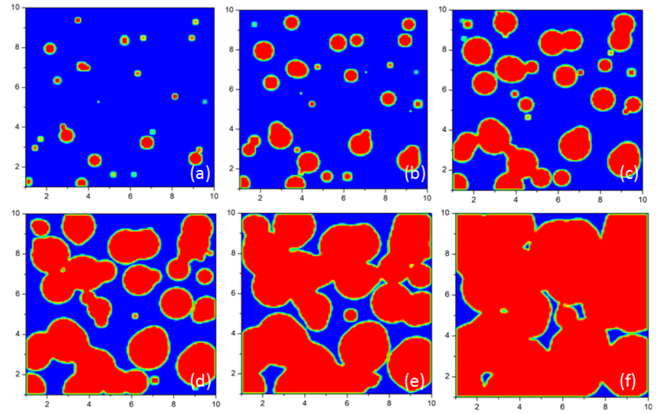

Figure 3 A typical example of the phase transformation process in the simulation with the parameters of VV=G=1, $d_{tt}=1$, $d_{xx}=d_{yy}=1/300$. (a) “new” phase coverage percentage X_T=3.968%, the non-dimensional time tt=21; (b) X_T=14.033%, tt=31 ; (c) X_T=32.518%, tt=41; (d) X_T=56.038%, tt=51; (e) X_T=78.551%, tt=61; (f) X_T= 93.322 %, tt=71

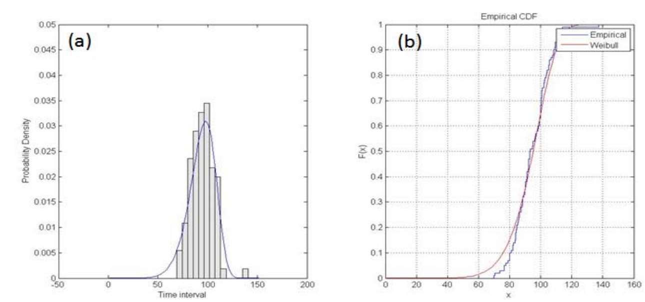

Figure 4 The PDF fitting (a) and CDF fitting (b) of TTFs (time of full coverage of “new” phase) scatter by Weibull distribution from 400 runs of simulation with the parameter of VV=G=1, $d_{tt}=1$, $d_{xx}=d_{yy}=1/300$

With the 100% failure criteria, in non-dimensional scale, the Weibull parameter a dependence on G is very well approximated by power dependence:

$$a \cong \frac{105}{VV^{2/3}} = 105\cdot\left(\frac{\nu L^3}{V}\right)^{2/3}.$$

The shape parameter β is much more sensitive to statistics. So far, for the case of 400 values of TTFs for each value of parameter G, the best approximation was

$$b \approx 8.0\cdot(G)^{-0.11} \approx b \approx 8.0\cdot(G)^{-1/9},$$

with the 100% failure criteria.

Coming back to the real time in seconds, we obtain the common Weibull distribution

$$F(tt) = 1 - \exp\left(-\left(\frac{t}{\eta}\right)^{\beta}\right)$$

with the scale parameter giving no contact size dependence,

$$\eta = a\frac{1}{\nu L^2} \cong 105 \cdot \left(\frac{\nu L^3}{V}\right)^{2/3} \frac{1}{\nu L^2} = \frac{105}{\left(\nu V^2\right)},$$

and the shape parameter giving rather simple size dependence of the shape parameter:

$$\beta \approx 8.0 \cdot G^{-1/9} = 8.0\left(\frac{\nu}{V}\right)^{1/9} L^{1/3} \cdot$$

From figure 5, we can find that a different failure criteria can change both scale parameter and shape parameter's dependences on G:

$$\eta = \frac{z}{\left(\nu V^2\right)},$$

$$z(100\%) \approx 105,\ z(90\%) \approx 63,\ z(80\%) \approx 55,$$

$$\beta \approx Q\left(\frac{\nu}{V}\right)^{m/3} L^m,$$

$$Q(100\%) \approx 8, m(100\%) \approx 1/3,$$

$$Q(90\%) \approx Q(80\%) \approx 12,$$

$$m(90\%) \approx m(80\%) \approx 1.$$

Summary

High resolution synchrotron radiation x-rays 3D imaging techniques, both tomography and laminography, were employed to study the EM failure mechanism in flip-chip solder joints. The observation of the early-stage damage evolution at the interface between UBM and solder balls, suggested that due to the increase of the thickness of UBM, the failure mode would turn from the gradual propagation of one pancake void to the stochastic nucleation and lateral growth of many voids which can be described by JMA kinetics model. Thus, we proposed JMA model could serve as a new physical model for life-time prediction of Pb-free solder joints in EM tests. A Monte Carlo simulation was developed to study this simplified failure model and the dependences of the scale parameter and shape parameter in the statistical Weibull equation on the physical factors of the EM tests were discussed. From the discussion, we can see that,

1) the characteristic time to failure, the scale parameter of the Weibull distribution, practically does not depend on the contact plane size;
2) on the contrary , the width of time to failure distribution increases with increasing contact size (increasing parameter $\frac{\nu L^3}{V}$), thus the shape parameter decreases. It means that indeed, in small contacts the danger of early failure becomes bigger.

Acknowledgments

The authors at UCLA would like to acknowledge the support from SRC contract KJ-1772. Tian would like to acknowledge Dr. Alastair MacDowell and Dr. Dula Parkinson for assistance in using beamline 8.3.2 at Advanced Light Source. The Advanced Light Source is supported by the Director, Office of Science, Office of Basic Energy Sciences, of the US Department of Energy, under Contract No. DE-AC02-05CH11231 at Lawrence Berkeley National Laboratory. We acknowledge the European Synchrotron Radiation Facility for provision of synchrotron radiation facilities and we would like to thank Dr. Marco di Michiel, Dr. Lukas Helfen, Dr. Feng Xu and Mr. Yin Cheng for assistance in using beamline ID15A.

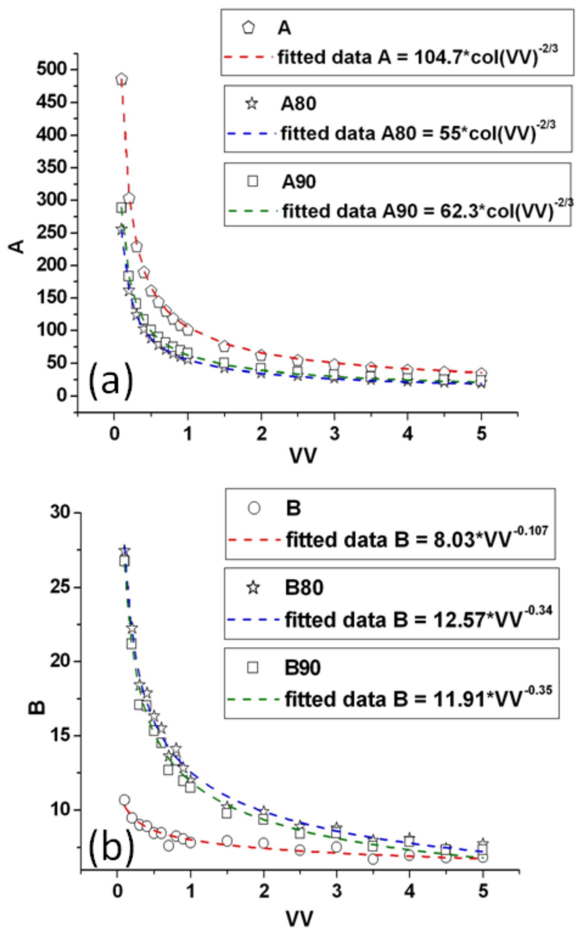

Figure 5 Dependence of a-parameter (a) and b-parameter (b) of Weibull distribution for non-dimensional TTFs on the non-dimensional parameter $G \equiv VV = V/\upsilon L^3$, with three different failure criteria (80%, 90%, 100%) , respectively.

Reference

1. K. N. Tu, "Recent advances on electromigration in very-large-scale-integration of interconnects," J. Appl. Phys., 94, 5451-5473 (2003)
2. Lingyun Zhang, Shengquan Ou, Joanne Huang, K.N.Tu, Stephen Fee, and Luu Nguyen, "Effect of current crowding on void propagation at the interface between intermetallic compound and solder in flip chip solder joints", Appl. Phys. Lett. 88, 012106 (2006)
3. Yao Yao, Leon M. Keer, and Morris E. Fine, "Electromigration effect on pancake type void propagation

near the interface of bulk solder and intermetallic compound", Journal of Applied Physics, 105, 063710 (2009)

4. Ming-Hwa R. Jen, Lee-Cheng Liu, and Yi-Shao Lai, "Modeling of electromigration on void propagation at the interface between under bump metallization and intermetallic compound in flip-chip ball grid array solder joints", Journal of Applied Physics 107, 093526 (2010)
5. Tian Tian, Kai Chen, A. A. MacDowell, Dula Parkinson, Yi-Shao Lai, and K. N. Tu, "Quantitative X-ray microtomography study of 3-C void growth induced by electronmigration in eutectic SnPb flip-chip solder joints", Scripta Materialia 65, 646 (2011).
6. Tian Tian, Feng Xu, Jung Kyu Han, Daechul Choi, Yin Cheng, Lukas, Helfen, Marco Di Michiel, Tilo Baumbach and K. N. Tu, "Rapid diagnosis of electromigration induced failure time of Pb-free flip chip solder joints by high resolution synchrotron radiation laminography", Applied Physics Letter 99, 082114 (2011)
7. J. H. Kinney, M. C. Nichols, "X-ray tomographic microscopy (XTM) using synchrotron radiation", Annu. Rev. Mater. Sci., 22 (1992), p. 121
8. L. Helfen, T. Baumbach, P. Mikulík, D. Kiel, P. Pernot, P. Cloetens and J. Baruchel, "High-resolution three-dimensional imaging of flat objects by synchrotron-radiation computed laminography", Appl. Phys. Lett. 86, 071915 (2005).
9. L. Helfen, T. Baumbach, P. Cloetens, and J. Baruchel, "Phase-contrast and holographic computed laminography", Appl. Phys. Lett. 94, 104103 (2009).